The Role of Polyamine Architecture on the Pharmacological Activity of Open Lactone Camptothecin−Polyamine Conjugates

ARTICLE *in* BIOCONJUGATE CHEMISTRY · NOVEMBER 2008

Impact Factor: 4.51 · DOI: 10.1021/bc800033r · Source: PubMed

12 AUTHORS, INCLUDING:

Greta Varchi
Italian National Research Council
69 PUBLICATIONS **540** CITATIONS
SEE PROFILE

Gabriele Fontana
Indena S.p.A.
94 PUBLICATIONS **1,606** CITATIONS
SEE PROFILE

Ezio Bombardelli
University of Milan
255 PUBLICATIONS **4,526** CITATIONS
SEE PROFILE

Jessica Fiori
University of Bologna
51 PUBLICATIONS **612** CITATIONS
SEE PROFILE

The Role of Polyamine Architecture on the Pharmacological Activity of Open Lactone Camptothecin−Polyamine Conjugates

Cristian Samor,*[,†] Andrea Guerrini,[†] Greta Varchi,[†] Giovanni Luca Beretta,[‡] Gabriele Fontana,[§] Ezio Bombardelli,[§] Nives Carenini,[‡] Franco Zunino,[‡] Carlo Bertucci,[||] Jessica Fiori,[||] and Arturo Battaglia[†]

Istituto CNR per la Sintesi Organica e Fotoreattività "I.S.O.F.", Area della Ricerca di Bologna, Via Gobetti 101, 40129 Bologna, Italy, Dipartimento di Oncologia Sperimentale e Laboratori, Fondazione IRCCS Istituto Nazionale Tumori, 20133 Milano, Italy, Indena SPA, viale Ortles 12, 20139 Milano, Italy, and Dipartimento di Scienze Farmaceutiche, Università di Bologna, Via Belmeloro 6, 40126 Bologna, Italy. Received January 25, 2008; Revised Manuscript Received August 19, 2008

A series of camptothecin open-ring lactone tripartate conjugates were synthesized, in which polyamine side chains with different architecture (ethane-1,2-diamine, spermidine, homospermidine, spermine, and 4,8,13,17-tetrazaicosane-1,20-diamine) are linked to the 21-carboxylic function through an amidic bond, while the 17-CH_2OH is acetylated. The rationale for the synthesis of these compounds was to explore the influence of the polyamine architecture on the activity of these CPT conjugates into cells, since the positively charged ammonium cations would favor interaction through electrostatic binding to the negatively charged DNA backbone. Topoisomerase I-mediated DNA cleavage assay was used to investigate the ability of these compounds to stimulate the DNA damage. The cleavage pattern was found to be similar to that of SN38 for all the new CPTs. The CPT tripartates were tested for growth inhibition ability against the human non-small-cell lung cancer carcinoma NCI-H460 cell line. Although these compounds were less potent than topotecan, SN38, and CPT after 1 h of treatment, the antiproliferative effects greatly increased after 72 h of exposure. The growth inhibition potency during long-term exposure is correlated with the number of charges of the 21-amide substituent. Both cleavage assay and *in vitro* effects support the interpretation that the compounds may have inhibitory activity also in the open-ring form. The architecture of the polyamine moiety is important for antiproliferative activity, and a balance between the hydrophilic and lipophilic properties of the polyamine is critical for CPT potency.

INTRODUCTION

Camptothecins (CPT, **1**, Figure 1) are an effective class of antitumor drugs, used in the treatment of a wide spectrum of human cancers. The molecular target of the CPTs family is the enzyme DNA topoisomerase I (topo I), a ubiquitous enzyme which is overexpressed in a variety of tumor cell lines and involved in the regulation of DNA topology during replication, recombination, and transcription (*1*−*4*). The drug stabilizes a reversible enzyme−DNA complex, which is termed the cleavable complex, thus preventing the ligation step of the enzyme action. These biochemical observations, integrated by crystallographic (*5*−*7*), UV−vis (*8, 9*), and NMR (*9*) spectroscopic information and quantum mechanic calculations (*9*−*14*), allowed the design of binding models for CPT with the covalent binary complex (*5, 11, 12, 15*).

Therapeutic applications of CPT have been limited by its low water solubility and by the high *in vivo* reactivity of the α-hydroxy-δ-lactone pharmacophore, which, under physiological conditions, reversibly hydrolyzes to the "ring-opened" carboxylate form (**1a**, Figure 1) (*16*). The latter is very toxic (*17*) and far less active with respect to inhibition of topo I (*18, 19*). In addition, the carboxylate form (**1a**) readily binds to human serum albumin, making it less accessible for cellular uptake (*20, 21*). This behavior gives rise to a drop in therapeutic efficacy, along with formulation difficulties (*21*). For these reasons, all the elements controlling the structure and lactone−carboxylate equilibrium are key factors in determine their potency. To avoid this inconvenience, a number of CPT analogues have been synthesized to improve lactone stability and aqueous solubility. These efforts have produced the two water-soluble semisynthetic analogues: topotecan (Hycamptin, **2**) (*22*) and irinotecan (Camptostar, **3**) (*23*), which received FDA approval for the clinical treatment of the ovarian, small-cell lung, and refractory colorectal cancers, while several other analogues are currently under development. Although **2** and **3** showed activity against a wide range of tumors, both of them have a relatively low therapeutic index and considerable toxic effects (*24*−*26*). In this regard, several prodrug strategies (*27*−*29*) have rapidly emerged to achieve site-specific delivery of

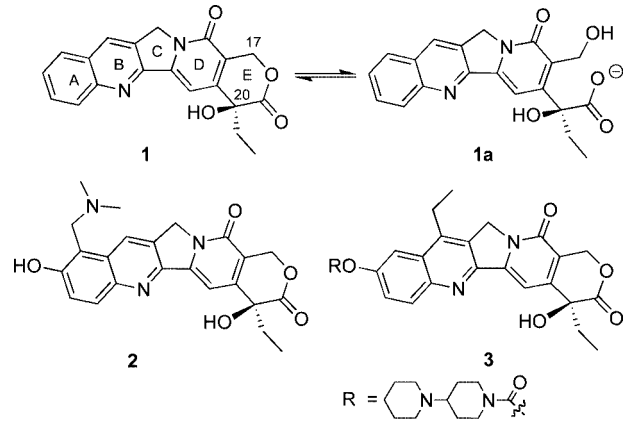

Figure 1. Camptothecin **1**, its carboxylate **1a**, and its FDA approved analogues Topotecan **2** and Irinotecan **3**.

* E-mail: csamori@isof.cnr.it. Phone: (039) 639-8286. Fax: (039) 6398349.
[†] I.S.O.F.
[‡] Fondazione IRCCS Istituto Nazionale Tumori.
[§] Indena SPA.
[||] Università di Bologna.

10.1021/bc800033r CCC: $40.75
Published on Web 10/08/2008

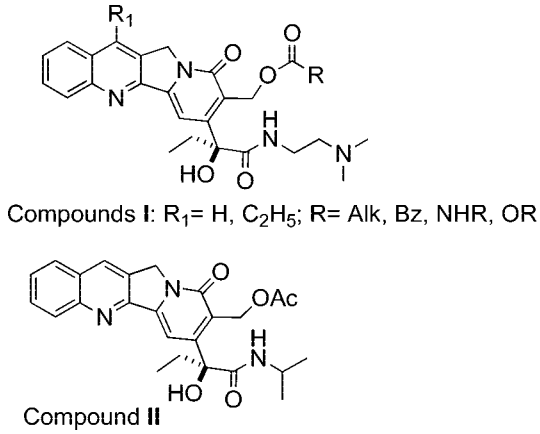

Figure 2. 21-N^1,N^1-dimethylaminoethylamide (compound **I**) and 21-isopropyl amide (compound **II**) tripartates.

cytotoxic CPTs. Most of these strategies are based on the use of conjugates that maintain CPT in the closed-lactone form into the plasma compartment. To this end, it is known that the free 20-hydroxyl group favors the lactone ring-opening through intramolecular hydrogen bonding (*30*). Therefore, acylation of the 20-hydroxyl group would render the lactone moiety more stable toward ring opening (*31*). Accordingly, 20(*S*)-*O*-acyl esters (*32, 33*), 20(*S*)-*O*-carbonated linked tripeptide conjugates (*34*), and 20(*S*)-*O*-linked glycoconjugates (*35*) were synthesized and showed excellent *in vitro* cytotoxicity. Alternatively, reactive functional groups, such as amino, hydroxyl, and carboxylic acid substituents, were introduced in the quinoline (A/B) ring system as linkers for ligand conjugation (*36*−*41*).

A scarcely explored family of CPT conjugates is the tripartate prodrugs, which are characterized by an E-ring open form, where the C-21 position is linked to a *carrier* by an amidic bond, while the 17-hydroxy group is acetylated. The synthesis of these conjugates relies on the fact that the 17-OH-21-amide CPT derivatives (dipartates) are sufficiently stable to allow the 17-OH acylation, yielding more stable ester−amide tripartates (*42*). These 17-*O*-acylated 21-amides, which are stable under physiological conditions for several hours, are supposed to act through a two-step mechanism: the acyl moiety undergoes enzymatic hydrolysis, affording the corresponding dipartate 17-CH_2OH-21-amides (*43*−*45*), subsequently, the free 17-OH group anchimerically assists the spontaneous amide hydrolysis, which generates the lactone species through cyclization. Although only a few examples have been reported in the literature, their biological data showed that their action strongly depends on the structure of both the ester and the amide moieties. For example, the inhibitory activity of CPT tripartates bearing an acyl ester, a carbonate, or a carbamate moiety at the 17 position and a N^1,N^1-dimethylaminoethylamide group at the 21 position (compound **I**, Figure 2) showed higher *in vivo* activity than the 7-ethylcamptothecinic sodium salt (*43, 44*). Instead, the 17-*O*-acyl esters of CPT tripartates bearing an isopropylamide substituent at the 21 position (compound **II**, Figure 2) showed lower *in vitro* and *in vivo* activity than camptothecinic sodium salt (*42, 43*). This behavior is due to the different hydrolytic profile of the amide group of their corresponding 17-CH_2OH dipartates. Actually, the amidic bond of compound **I** hydrolyzes very rapidly at physiological pH, while the isopropyl amide group (compound **II**) hydrolyzed very slowly, being the rate-determining step in the generation of the lactone species.

Besides compounds of types **I** and **II**, two very efficient CPT PEGylate tripartates were reported (**4** and **5**, Figure 3), which show little *in vitro* efficacy in tissue cultures (*45*).

According to the authors, an initial rapid hydrolysis of the ester (or carbonate) affords the corresponding relatively stable and nonactive dipartates. Therefore, cyclization to the active lactone species, which occurs only within the tumor environment, is the rate-determining step (*46*).

The tripartate reactivity scenario is further complicated when considering the possibility that these compounds may exhibit intrinsic antitumor activity. Our recent results regarding the water-soluble CPT tripartate **6** (Figure 4) showed that this compound and its analogues maintain the same order of potency of their reference CPTs, despite the E ring opened form (*47*).

These results cannot be ascribed to the derivative lactonization, since no free CPT was recovered at the end of DNA cleavage assays, and the low amount of CPT detectable in plasma and tumor did not account for the observed efficacy. Thus, these 17-acetate-21 spermidine derivatives could represent the first example of an effective CPT drug with opened lactone ring.

To provide novel insights into this class of open-lactone conjugates, we have synthesized a family of 17-O-acyl protected tripartates of CPT bearing polyamines at the C21-carboxyl group. The ubiquitous polyamines, such as cadaverine, putrescine, spermidine, and spermine, are biosynthesized in humans and play an essential role as regulators of cell growth and differentiation (*48*−*50*). Many tumor types contain high levels of polyamines and an activated exogenous polyamines transporter (PAT) (*51*). Polyamines are organic cations, since the primary and secondary amino groups are protonated at physiological pH. The unique feature of polyamine structure is the presence of methylene groups, which favor hydrophobic interactions, and the presence of positive charges at defined distances, which can electrostatically interact with negatively charged DNA (*52*). In addition to this charge neutralization, polyamines interact with nucleic acid bases, dock into the major or minor grooves, and enter into multisite interactions depending on the ionic environment (*53, 54*). However, the mechanism of polyamine entry into mammalian cells remains poorly defined (*55*−*57*), and more data are needed on the transporters that are believed to facilitate specific delivery to tumor cells, in order to design proper prodrugs. Nevertheless, several attempts to design a polyamine vector have been reported, which are based on structure−activity studies aimed at explaining which polyamine sequence would be the most suitable to access the transporter (*58*−*62*). These studies suggest that small structural changes in the polyamine skeleton give rise to strong differences in their transport behavior and that linear polyamines are superior vectors to the branched ones (*54, 63*−*69*).

MATERIALS AND METHODS

General. All reactions were performed under an atmosphere of dry nitrogen using oven-dried glassware. Tetrahydrofuran, toluene, and ethyl ether were distilled from sodium benzophenone ketal. Dichloromethane and DMF were distilled from calcium hydride. All other solvents were HPLC grade. Reactions were magnetically stirred and monitored by thin-layer chromatography (TLC) with E. Merck silica gel 60-F254 plates. Flash column chromatography was performed with Merck silica gel (0.04−0.63 μm, 240−400 mesh) under high pressure. NMR spectra were recorded on a 400 MHz spectrometer. Unless otherwise stated, all NMR spectra were measured in $CDCl_3$ solutions and referenced to the $CHCl_3$ signal. All ^{1}H and ^{13}C shifts are given in ppm (s = singlet; d = doublet; t = triplet; dd = quadruplet; dt = doublet of triplets, m = multiplet; br s = broad signal). Coupling constants *J* are given in Hz. Assignments of proton resonances were confirmed, when possible, by selective homonuclear decoupling experiments or by correlated spectroscopy. IR spectra were recorded on a FT-IR ESP spectrometer as thin films on NaCl plates. Mass spectra were recorded on an ion trap spectrometer with an ionization

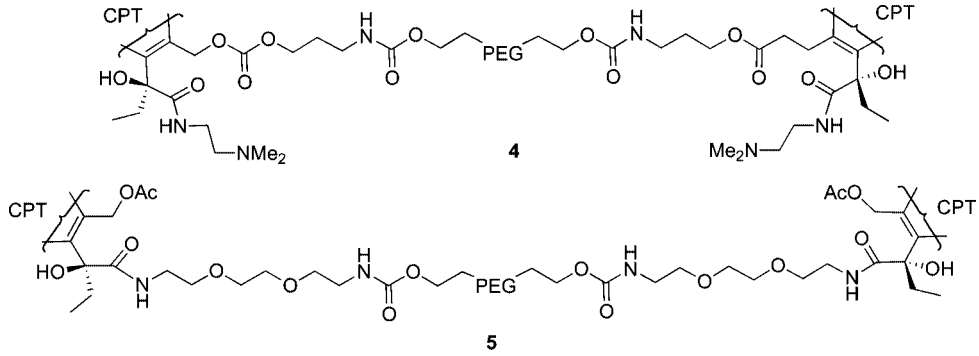

Figure 3. PEG-Tripartates **4** and **5**.

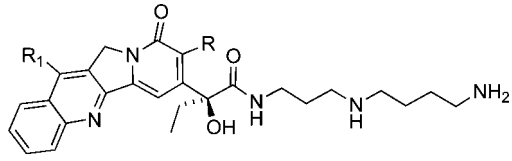

Figure 4. Compounds **6** and **7**.

potential of 70 eV. High-resolution mass spectra (HRMS) were performed with a resolution of 10 000 against a suitable mass standard. The commercially available reagents were used as received without further purification.

General Procedure. For the synthesis of tripartate conjugates **18**, **7**, and **19** from CPT **1** and *N*-^{t}BOC polyamines **13**, **14**, and **16**, respectively, CPT **1** (1.0 equiv), was suspended in 5.0 mL of dry pyridine, and the *N*-*t*BOC-polyamines **13**, **14**, and **16** (4.0 equiv) were added. The reaction was heated at 80 °C for 70 h, and than the solvent was removed under reduced pressure. Flash chromatography, CH_2Cl_2−MeOH (30:1), of the crude material afforded the derivatives 17-hydroxy-21-Boc-amides in 88%, 55%, and 10% yields, respectively, as yellow solids. These compounds (1.0 equiv) were dissolved in dry pyridine (5.0 mL), and acetic anhydride (20.0 equiv) was added. The reaction mixture was magnetically stirred for 2 h at 20 °C, and then the excess of solvent and reagent were removed under vacuum. The resulting solid residue was purified by silica gel flash chromatography, CH_2Cl_2−MeOH (30:1), affording the corresponding 17-*O*-acyl-21-*N*-^{t}Boc-amides in quantitative yield. To a cooled solution (0 °C) of these conjugates (1.0 equiv) in dry DCM (8.0 mL), TFA (15.7 equiv) was added dropwise with stirring over a period of 30 min. The reaction was stirred for 60 h at 0−4 °C, and then the solvent was removed under reduce pressure to obtain the tripartates **18**, **6**, and **19**, respectively, as pale yellow solids.

Compound 18. (88%); pale yellow solid. HRMS *m*/*z* calcd for $C_{26}H_{27}F_3N_4O_7$ $[M]^+$ 564,1832; *m*/*z* found 564,1841. ^{1}H NMR (400 MHz, DMSO-d_6/D_2O) δ 8.58 (s, 1 H, Ar), 8.08 (d, 1 H, J = 8.4 Hz, Ar), 8.01 (d, 1 H, J = 8.4 Hz, Ar), 7.81 (t, 1 H, J = 8.4 Hz, Ar), 7.64 (t, 1 H, J = 8.4 Hz, Ar), 7.53 (s, 1 H, Ar), 5.29 (d, 1 H, J = 11.2 Hz), 5.20 (d, 1 H, J = 11.2 Hz), 5.15 (s, 2 H, H-5), 3.38 (m, 1 H), 3.22 (m, 1 H), 2.86 (bt, 2 H), 2.22 (m, 1 H), 2.13 (m, 1 H), 1.95 (s, 3 H), 0.87 (t, 3 H, J = 7.8 Hz). ^{13}C NMR (100 MHz, DMSO-d_6) δ 174.1, 171.0, 161.3, 156.2, 153.4, 148.6, 144.9, 132.3, 131.1, 130.7, 129.7, 129.2, 128.7, 128.3, 123.9, 99.4, 79.3, 59.4, 51.0, 38.9, 37.3, 32.4, 21.4, 8.5.

Compound 6. (55%); pale yellow solid. HRMS *m*/*z* calcd for $C_{33}H_{39}F_6N_5O_9$ $[M]^+$ 763,2652; *m*/*z* found 763,2644. ^{1}H NMR (400 MHz, DMSO-d_6/D_2O) δ 8.63 (s, 1 H, Ar), 8.12 (d, 1 H, J = 8.4 Hz, Ar), 8.05 (d, 1 H, J = 8.4 Hz, Ar), 7.86−7.81 (m, 1 H, Ar), 7.70−7.65 (m, 1 H, Ar), 7.50 (s, 1 H, Ar), 5.29 (d, 1 H, J = 11.2 Hz, H-17), 5.24 (d, 1 H, J = 11.2 Hz, H-17), 5.21 (s, 2 H, H-5), 3.20−3.00 (m, 2 H), 2.88−2.80 (m, 4 H), 2.80−2.72 (m, 2 H), 2.18−2.28 (m, 1 H), 2.06−2.18 (m, 1 H), 1.95 (s, 3 H), 1.76−1.66 (m, 2 H), 1.60−1.48 (m, 4 H), 0.88 (t, 3 H, J = 7.8 Hz). ^{13}C NMR (100 MHz, DMSO-d_6) δ 173.9, 171.0, 161.3, 158.0 (q, CO_2H of TFA), 156.5, 153.4, 148.7, 144.9, 132.3, 131.1, 130.6, 129.7, 1292, 128.7, 128.3, 124.0, 99.5, 79.4, 59.5, 51.0, 46.8, 45.3, 38.9, 36.7, 32.3, 26.5, 24.8, 23.3, 21.4, 8.6.

Compound 19. (10%); pale yellow solid. HRMS *m*/*z* calcd for $C_{38}H_{47}F_9N_6O_{11}$ $[M]^+$ 934,3159; *m*/*z* found 934,3168. ^{1}H NMR (400 MHz, CD_3OD) δ 8.65 (s, 1 H, Ar), 8.18 (d, 1 H, J = 8.4 Hz, Ar), 8.07 (d, 1 H, J = 8.4 Hz, Ar), 7.88 (t, 1 H, J = 8.4 Hz, Ar), 7.83 (s, 1 H, H-14), 7.72 (t, 1 H, J = 8.4 Hz, Ar), 5.46 (d, 1 H, J = 11.2 Hz, H-17), 5.40 (d, 1 H, J = 11.2 Hz, H-17), 5.33 (s, 2 H, H-5), 3.18−3.00 (m, 12 H), 2.48−2.40 (m, 1 H, H-19), 2.34−2.26 (m, 1 H, H-19), 2.12−2.08 (m, 4 H), 2.06 (s, 3 H), 1.90−1.76 (m, 4 H), 1.06 (t, 3 H, J = 7.6 Hz). ^{13}C NMR (100 MHz, CD_3OD) δ 176.4, 173.2, 163.3, 158.5, 153.8, 149.7, 146.2, 133.4, 132.0, 131.0, 130.0, 129.8, 129.7, 129.1, 125.5, 102.2, 80.0, 60.5, 51.8, 46.7, 46.3, 45.9, 37.8, 37.1, 36.8, 33.2, 27.7, 27.5, 25.4, 24.3, 22.4, 8.3.

17-Acetylcamptothecin-21-benzylamide (*21*). CPT **1** (350 mg, 1.01 mmol), was suspended in dry benzyl amine (2.5 mL). The reaction mixture was heated at 45−50 °C for 2.5 h, and then the solvent was removed under reduced pressure. Water was then added, and the aqueous layer was extracted with CH_2Cl_2 (15 mL × 3). The combined organic extracts were dried over anhydrous Na_2SO_4, filtered, and concentrated under vacuum to afford 17-hydroxy-21-benzylamide as a yellow solid (440 mg, 96%). The crude material was used for the next step without further purification.

17-hydroxy-21-benzylamide (440 mg, 0.97 mmol) was dissolved in dry pyridine (10 mL), and acetic anhydride (1.8 mL, 19.4 mmol) was added. The reaction was stirred at room temperature until TLC analysis [CH_2Cl_2−MeOH (30:1)] showed complete consumption of the starting material (2.5 h). The solvent and the excess of reagent were then removed under vacuum, and water was added. The aqueous layer was extracted with CH_2Cl_2 (20 mL × 3). The organic layer was further washed with 5% HCl and dried over anhydrous Na_2SO_4, filtered, and concentrated in vacuo to afford **21** (480 mg, ∼100%) in quantitative yield as a pale yellow solid. HRMS *m*/*z* calcd for $C_{29}H_{27}N_3O_5$ $[M]^+$ 497,1951; *m*/*z* found 497,1964. ^{1}H NMR (400 MHz, $CDCl_3$) δ 8.19 (s, 1 H, Ar), 8.11 (d, 1 H, J = 8.4 Hz, Ar), 7.74 (t, 1 H, J = 8.4 Hz, Ar), 7.69 (d, 1 H, J = 8.4 Hz, Ar), 7.63 (s, 1 H, H-14), 7.51 (t, 1 H, J = 8.4 Hz, Ar), 7.35−7.20 (m, 5 H, Ar), 5.56 (d, 1 H, J = 12.0 Hz), 5.44 (d, 1 H, J = 12.0 Hz), 5.19 (d, 1 H, J = 16.4 Hz), 5.13 (d, 1 H, J = 16.4 Hz), 5.13 (s, 1 H, O*H*), 4.53 (dd, 1 H, J_1 = 4.8 Hz, J_1 = 6.4 Hz), 4.39 (dd, 1 H, J_1 = 14.8 Hz, J_1 = 6.4 Hz), 2.56−2.46 (m,

1 H, H-19), 2.38−2.28 (m, 1 H, H-19), 2.04 (s, 3 H), 1.08 (t, 3 H, $J = 7.6$ Hz). ^{13}C NMR (100 MHz, $CDCl_3$) δ 172.1, 171.1, 161.5, 157.0, 151.3, 148.0, 144.1, 137.7, 130.5, 130.1, 128.9, 128.6, 128.5, 128.0, 127.8, 127.7, 127.5, 127.2, 124.9, 100.7, 78.5, 58.7, 50.3, 43.5, 33.1, 20.9, 7.9.

17-Acetylcamptothecin-21-benzyl Ester (*23*). To a solution of **21** (480 mg, 0.97 mmol) in a 2:1 mixture of Ac_2O (12 mL) and AcOH (6 mL) was added granular $NaNO_2$ (1.34 g, 19.4mmol) in portions over 2 h at 0−4 °C. Evolution of brown gas occurred. The flask was kept in the ice bath for 2 h and allowed to warm to room temperature and further reacted for 24 h. The mixture was then poured into ice/water and extracted with CH_2Cl_2 (3×). The combined organic layers were washed with 5% Na_2CO_3 followed by H_2O and dried over Na_2SO_4. Evaporation of solvent afforded compound **22** as yellowish solid, which was immediately dissolved with anhydrous 1,4-dioxane (16 mL) and refluxed for 5 h. The reaction mixture was cooled to room temperature, and the solvent was removed under vacuum to give **23** (483 mg, ≈100%). The crude product was sufficiently pure for the following step. However, an analytical sample of **23** was purified by silica gel flash chromatography CH_2Cl_2−MeOH (30:1). **23**: HRMS *m*/*z* calcd for $C_{29}H_{26}N_2O_6$ $[M]^+$ 498,1791; *m*/*z* found 498,1798. ^{1}H NMR (400 MHz, $CDCl_3$) δ 8.33 (s, 1 H, Ar), 8.20 (d, 1 H, $J = 8.4$ Hz, Ar), 7.89 (d, 1 H, $J = 8.4$ Hz, Ar), 7.80 (t, 1 H, $J = 8.4$ Hz, Ar), 7.63 (t, 1 H, $J = 8.4$ Hz, Ar), 7.52 (s, 1 H, H-14), 7.33−7.24 (m, 5 H, Ar), 5.50 (d, 1 H, $J = 11.6$ Hz), 5.47 (d, 1 H, $J = 11.6$ Hz), 5.29 (d, 1 H, $J = 12.0$ Hz), 5.23 (s, 2 H), 5.16 (d, 1 H, $J = 12.0$ Hz), 4.32 (s, 1 H, O*H*), 2.41−2.24 (m, 2 H, H-19), 2.03 (s, 3 H), 0.95 (t, 3 H, $J = 7.6$ Hz). ^{13}C NMR (100 MHz, $CDCl_3$) δ 173.5, 171.0, 161.4, 153.4, 152.5, 148.7, 144.7, 134.7, 131.0, 130.5, 129.5, 128.8, 128.6, 128.6, 128.3, 128.1, 128.1, 127.8, 124.9, 99.8, 79.4, 68.2, 58.7, 50.2, 32.2, 20.9, 7.6.

17-Acetylcamptothecinic Acid (*20*). Crude **23** (226 mg, 0.45 mmol) was dissolved in THF−EtOH (1:1). Dry 10% Pd/C (48 mg) was carefully added to the reaction mixture, and the dissolved oxygen was removed under vacuum. Then, a balloon of hydrogen was mounted, and the mixture was stirred for 10 h at room temperature. The catalyst was removed by filtration through a celite pad, and the filtrate was concentrated under vacuum. The crude material was purified by silica gel flash chromatography CH_2Cl_2−MeOH (step gradient elution 20:1, 10:1) to afford **20**. HRMS *m*/*z* calcd for $C_{22}H_{20}N_2O_6$ $[M]^+$ 408,1321; *m*/*z* found 408,1330. ^{1}H NMR (400 MHz, DMSO-d_6) δ 8.64 (s, 1 H, Ar), 8.18 (d, 1 H, $J = 8.4$ Hz, Ar), 8.08 (d, 1 H, $J = 8.4$ Hz, Ar), 7.85−7.81 (m, 2 H, Ar), 7.68 (t, 1 H, $J = 8.4$ Hz, Ar), 5.90 (s, 1 H, O*H*), 5.61 (d, 1 H, $J = 10.4$ Hz), 5.39 (d, 1 H, $J = 10.4$ Hz), 5.20 (s, 2 H), 1.98−1.82 (m, 5 H, H-19 + Me), 0.82 (t, 3 H, $J = 7.6$ Hz). ^{13}C NMR (100 MHz, DMSO-d_6) δ 171.0, 161.8, 160.0, 153.9, 148.7, 143.5, 132.0, 130.9, 130.6, 129.7, 129.1, 128.5, 128.1, 123.6, 101.3, 80.6, 60.2, 50.6, 33.8, 21.5, 9.6.

General Procedure. For the preparation of tripartate conjugates **24**, **19**, and **25** from the addition reaction of **20** to N-^{t}BOC polyamines **15**, **16**, and **17**, respectively, to a solution of **20** (1 equiv) in dry DMF (2 mL) the polyamine (2 equiv) and Et_3N (3 equiv) were sequentially added. The reaction mixture was cooled at 0 °C and 1-[3-(dimethylamino)propyl]-3-ethylcarbodiimide hydrochloride (EDCI.HCl, 2.2 equiv) and *N*-hydroxybenzotriazole (HOBt, 2.1 equiv) were added. The mixture was stirred at 0 °C for 2 h, then warmed at 20 °C and reacted further for 40−50 h. The solvent was removed under reduced pressure, and the crude material was purified by silica gel flash chromatography in CH_2Cl_2−MeOH (step gradient elution 40:1, 30:1, and 15:1), to afford the corresponding 17-acetyl-21-*N*-^{t}BOC protected amides in 62%, 50%, and 27% yields, respectively. To a solution of these conjugates (1 equiv), in DCM (8 mL) TFA (15.7 equiv) was added dropwise at 0 °C. The solution was stirred for 60 h at 0−4 °C, and then solvents were removed under reduced pressure to afford the desire products **24**, **19**, and **25**, as pale yellow solids.

19: (50%); pale yellow solid.

Compound 24. (62%); pale yellow solid. HRMS *m*/*z* calcd for $C_{34}H_{43}F_6N_5O_9$ $[M]^+$ 779,2965; *m*/*z* found 779,2972. ^{1}H NMR (400 MHz, CD_3OD) δ 8.59 (s, 1 H, Ar), 8.13 (d, 1 H, $J = 8.4$ Hz, Ar), 8.02 (d, 1 H, $J = 8.4$ Hz, Ar), 7.83 (t, 1 H, $J = 8.4$ Hz, Ar), 7.78 (s, 1 H, H-14), 7.68 (t, 1 H, $J = 8.4$ Hz, Ar), 5.46 (d, 1 H, $J = 11.2$ Hz, H-17), 5.39 (d, 1 H, $J = 11.2$ Hz, H-17), 5.25 (s, 2 H, H-5), 3.10−2.90 (m, 8 H), 2.54−2.44 (m, 1 H, H-19), 2.33−2.24 (m, 1 H, H-19), 2.06 (s, 3 H), 1.82−1.66 (m, 8 H), 1.07 (t, 3 H, $J = 7.6$ Hz). ^{13}C NMR (100 MHz, CD_3OD) δ 174.5, 172.1, 162.2, 157.6, 152.5, 148.4, 144.8, 132.1, 130.7, 129.7, 128.7, 128.6, 128.5, 127.9, 124.5, 101.1, 78.7, 59.3, 50.5, 47.3, 46.9, 38.8, 38.4, 32.1, 26.3, 24.4, 23.5, 23.1, 21.4, 7.1.

Compound 25. (27%); pale yellow solid. HRMS *m*/*z* calcd for $C_{47}H_{63}F_{15}N_8O_{15}$ $[M]^+$ 1264,4173; *m*/*z* found 1264,4165. ^{1}H NMR (400 MHz, CD_3OD) δ 8.60 (s, 1 H, Ar), 8.14 (d, 1 H, $J = 8.4$ Hz, Ar), 8.03 (d, 1 H, $J = 8.4$ Hz, Ar), 7.85 (t, 1 H, $J = 8.4$ Hz, Ar), 7.80 (s, 1 H, H-14), 7.69 (t, 1 H, $J = 8.4$ Hz, Ar), 5.46 (d, 1 H, $J = 11.2$ Hz, H-17), 5.40 (d, 1 H, $J = 11.2$ Hz, H-17), 5.27 (s, 2 H, H-5), 3.18−3.00 (m, 20 H), 2.48−2.40 (m, 1 H, H-19), 2.34−2.26 (m, 1 H, H-19), 2.18−2.07 (m, 8 H), 2.06 (s, 3 H), 1.90−1.76 (m, 4 H), 1.06 (t, 3 H, $J = 7.6$ Hz). ^{13}C NMR (100 MHz, CD_3OD) δ 176.4, 173.2, 163.4, 158.4, 153.7, 149.6, 146.1, 133.3, 131.9, 131.0, 130.9, 129.9, 129.8, 129.7, 129.1, 125.5, 102.2, 80.0, 60.4, 51.7, 48.2, 46.8, 46.4, 45.9, 45.8, 45.8, 37.8, 37.1, 33.3, 30.9, 27.7, 27.5, 25.3, 24.1(2 C), 21.0, 8.3.

Growth Inhibition Assays. Human non-small-cell lung cancer NCI-H460 cells were cultured in RPMI 1640 containing 10% FCS. Cell sensitivity was assessed by growth inhibition assay after 1 or 72 h of drug exposure. Cells in the logarithmic phase of growth were seeded in duplicates into six-well plates. Twenty-four hours later, cells were exposed to the drug and counted with a Coulter counter 72 h after the beginning of drug exposure for 1 h of treatment and at the end of drug exposure in the case of 72 h of treatment. IC_{50} is defined as the inhibitory drug concentration causing a 50% decrease of cell growth over that of the untreated control.

Topoisomerase I-Dependent DNA Cleavage Assays. A gel-purified 751-bp *Bam*HI-*EcoRI* fragment of SV40 DNA was used for the cleavage assay (*1*). DNA fragments were uniquely 3′-end-labeled. Topoisomerase I-DNA cleavage reactions (20 000 cpm per sample) were done in 20 μL of 10 mM Tris-HCl (pH 7.6), 150 mM KCl, 5 mM $MgCl_2$, 15 μg/mL bovine serum albumin, 0.1 mM DTT, and the human recombinant enzyme (full-length topoisomerase I) for 30 min at 37 °C. Reactions were stopped using 0.5% SDS and 0.3 mg/mL of proteinase K for 45 min at 42 °C. Persistence of DNA cleavage at different time points was examined by adding 0.6 M NaCl after 30 min of incubation with 10 μM drug. After precipitation, DNA was resuspended in denaturing buffer (80% formamide, 10 mM NaOH, 0.01 mM EDTA, and 1 mg/mL dyes) before loading on a denaturing 8% polyacrylamide gel in Tris-borate EDTA buffer. Overall, DNA cleavage levels were measured with a PhosphoImager 425 mode (*2*).

Stability of Compound 18 in Cell Culture Medium and DNA Cleavage Buffer. The stability study was performed by using high-performance liquid chromatography (HPLC) coupled with mass spectrometry (LC-MS). In order to optimize the method, MS analyses in direct infusion mode were carried on a LCQ-Duo mass spectrometer (ThermoFinnigan, San Jose, CA), equipped with an electrospray ionization source (ESI),

operating in positive polarity under the following condition: spray voltage 4.5 kV, capillary temperature 200 °C. The mass spectra were recorded in total ion current (TIC) within 150 and 2000 *m/z* and in tandem mass modality (MS/MS). Quantitative LC-MS analyses of the cell culture media diluted 1:10 with 0.1% formic acid/acetonitrile 85:15 (v/v) were conducted on a Cap-LC liquid chromatograph interfaced with a Q-TOF hybrid mass analyzer (Micromass, Manchester, UK). Q-TOF micro was employed with a Z-spray ion source (source condition: capillary voltage 3.0 kV, source temperature 90 °C, desolvation temperature 250 °C). Chromatograms were acquired in the *m/z* range 100−600 (TIC modality). Reverse-phase chromatographic separations were obtained on a C18 Waters symmetry column (150 × 0.3 mm I.D., 3.5 μm), assembled with a security guard column (Waters Symmetry 300, C18 5 μm, NanoEase), using a gradient elution from A [water/acetonitrile/formic acid 95:5:0.1 (v/v/v)]/B [acetonitrile/water/formic acid 95:5:0.1 (v/v/v)] 80:20 (v/v), for 10 min, to A/B 10:90 (v/v), within 15 min, up to 25 min, to A/B 80:20 (v/v) within 25.10 min. Equilibration time at A/B 80:20 (v/v) was 15 min. The flow rate was 4.0 μL/min, and the injection volume was 0.3 μL.

Cell culture media (RPMI 1640 plus 10% FCS) containing 50 μM of compound **18**, after 1 and 72 h of incubation at 37 °C, and cleavage buffer (10 mM Tris-HCl (pH 7.6), 150 mM KCl, 5 mM $MgCl_2$, 15 μg/mL bovine serum albumin, 0.1 mM DTT) containing 50 μM of **18** after 1 h of incubation at 37 °C, were diluted 1: 10 with a mixture of 0.1% formic acid/acetonitrile 85:15 and analyzed by LC-Q-TOF system. To test whether the cell metabolism influences the E-ring closure of **18**, NCI-H460 cells (6×10^5) were seeded in cell culture flask (75 cm^2) and treated 24 h later with compound **18** for 1 h at the concentration corresponding to the IC_{80} value (about 60 μM). After 1 h exposure, cells and culture medium were immediately recovered and analyzed.

The analyses of standard compound **18** performed on the LCQ-Duo (see Supporting Information, Figure 8) showed the in-source fragmentation of its parent ion $[M + H]^+$ at 451.25 *m/z* to the main daughter ion at *m/z* 391.07. This fragmentation was confirmed by MS/MS analysis on the ion at *m/z* 451.25. The analyses on the LC-Q-TOF system (see Supporting Information, Figure 9) gave a more extensive in-source fragmentation, leading to the complete disappearance of compound **18** parent ion and the formation of the main fragment at 391.1938 *m/z* (exact mass) and other minor fragment at *m/z* 374.1770, 356.1726. CPT, a possible degradation product of **18**, was also analyzed by LC-MS ($[M + H]^+$ at 349.1090 *m/z*), and it was revealed in compound **18** standard solution as an impurity (3.66%). For calibration, five solutions of **18** (1.142 × 57.10 μM) were analyzed [equation curve: $y = 3.130 \pm 0.02112)x + 0.3937(\pm 0.5535)$; $r^2 = 0.9999$]; the limit of quantitation (LOQ) was measured at the concentration of 0.571 μM.

CHEMISTRY

To optimize the efficiency of this novel family of open-lactone ring CPTs, we explored the influence of the polyamine architecture on the activity of these CPT conjugates into cells. Since the molecular recognition events involved in polyamine transport are sensitive to the number of nitrogens present in the molecule and to the distance between them (*64, 65*), the following polyamine scaffolds were selected for our investigation: ethane-1,2-diamine **8**, spermidine **9**, homospermidine **10**, spermine **11**, and 4,8,13,17-tetraza-icosane-1,20-diamine **12** (Figure 5).

Direct amidation of CPT **1** with N-protected polyamines **13**, **14** (*70*), **16** (*71*) was performed in pyridine at 80 °C according to a modified Adamovics's protocol (*42*) (Scheme 1). Sequential

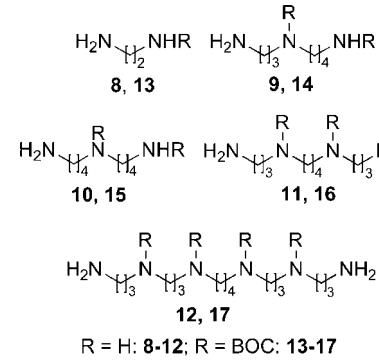

Figure 5. Structures of polyamines **8**−**12** and their correponding N-BOC derivatives **13**−**17**.

Scheme 1. Reactions of CPT with Polyamines

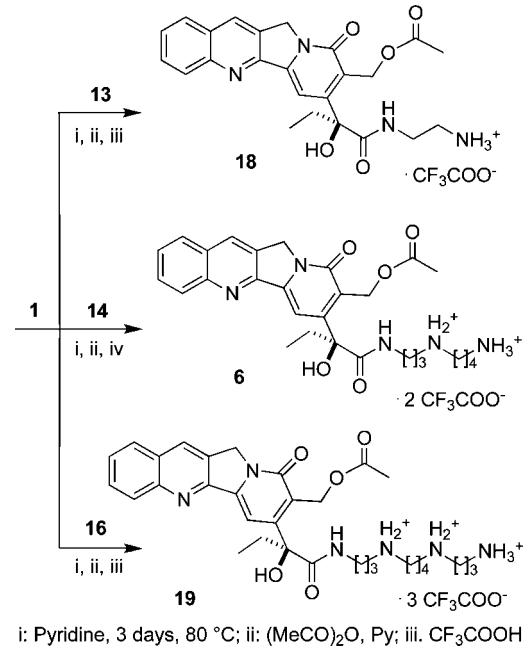

Scheme 2. Synthesis of 17-*O*-Acyl Protected Camptothecinic Acid 20

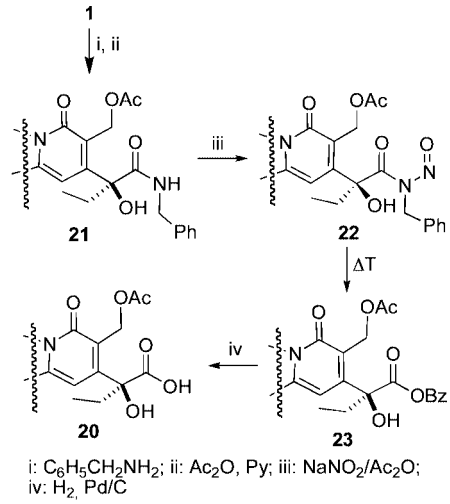

17-OH esterification of the resulting amides with Ac_2O followed by deprotection of the polyamine with trifluoroacetic acid afforded the tripartate conjugates **18**, **6**, and **19** as ammonium trifluoroacetates. Chemical yields of CPT amidation decreased with the enhancement of the polyamine length. For instance,

Scheme 3. Synthesis of Tripartates 19, 24, and 25

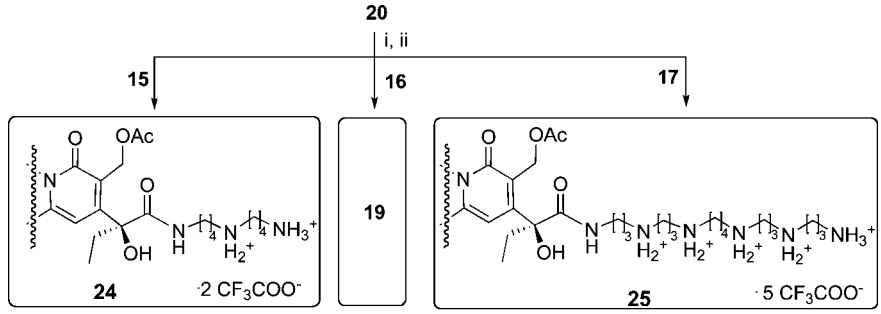

Table 1. Antiproliferative Activity of Camptothecin Derivatives on H460 Cells.[a]

	1 h exposure	72 h exposure	F.I.[b]
Topotecan	1.18 ± 0.24	0.015 ± 0.0027	79
SN38	0.22 ± 0.013	0.012 ± 0.001	18
CPT	0.18 ± 0.01	0.0059 ± 0.0024	30
18	6.04 ± 1.97	0.0023 ± 0.0004	2600
6	3.66 ± 0.34	0.048 ± 0.0075	76
19	2.1 ± 1.85	0.077 ± 0.019	28
24	7.7 ± 3.6	0.12 ± 0.03	64
25	1.44 ± 0.38	0.17 ± 0.027	8.5

[a] Sensitivity was assessed by growth inhibition assay after 1 or 72 h of drug exposure. Cells were counted 72 h after drug exposure for 1 h of treatment and at the end of drug exposure in the case of 72 h of treatment. The reported values are the mean ± SD of three independent experiments. [b] Fold increase: ratio between IC_{50} (μM) at 1 h and IC_{50} at 72 h.

chemical yields for the amidation of **1** were 88% and 55%, with the *N*-BOC derivatives **13** and **14**, respectively, but dropped to 10% when the spermine derivative **16** was used, while the coupling of CPT with polyamine **17** failed.

Such failure, along with the poor yields in the formation of compound **19**, prompted us to explore a more efficient protocol for the amidation reaction. We reasoned that 17-O-acyl camptothecinic acid **20** could be a suitable precursor for the synthesis of our tripartates. It has been reported that this naturally occurring compound can be either isolated from *Nothapodytes fetida* or obtained by acetylation of the corresponding sodium salt of **1** with Ac_2O in DMF (*72*). In our hands, this semisynthetic route was not reproducible, affording compound **20** in very low yield (<10%). Thus, we developed a new high-yielding and reproducible four-step synthesis, which afforded **20** in 80% starting from CPT. This methodology involves the one-pot sequential amidation of **1** with benzylamine, followed by acetylation of the free 17-OH group with acetic anhydride which provides the amide derivative **21** (Scheme 2).

Nitrosation of **21** with $NaNO_2$, in the presence of a mixture of Ac_2O and AcOH, afforded the corresponding *N*-nitroso amide **22**, which thermally rearranged to the benzylic ester **23**. Reductive debenzylation with H_2/Pd produced the target compound **20** in more than 80% overall yield. Amidation of **20** with **15**, **16**, and **17** (*73*) was performed according to a standard coupling procedure, using 1-ethyl-3-(3-dimethylaminopropyl) carbodiimide hydrochloride, in the presence of 1-hydroxybenzotriazole (Scheme 3). TFA removal of the *tert*-butoxy carbonyl protecting groups afforded the target conjugates **24**, **19**, and **25** as the trifluoroacetate salts.

BIOCHEMICAL ADN BIOLOGICAL EVALUATION

The CPT analogues were tested for growth inhibition ability against the human non-small-cell lung cancer carcinoma NCI-H460 cell line (Table 1) (*74*). The reduced potency of polyamine CPT derivatives with respect to topotecan, SN38, and CPT is likely related to the limited drug uptake, caused by their water-soluble salt formulation.

Although CPT derivatives were less potent than topotecan, SN38, and CPT after 1 h treatment, their antiproliferative effects increased after 72 h exposure. During long-term exposure, growth inhibition potency of **18** was higher than that of the reference drugs. Topoisomerase I-mediated DNA cleavage assay was carried out to investigate the ability of the compounds to stimulate DNA damage. Purified human topo I was used with SN38 as a reference compound (Figure 6A). Compound **18** exhibited DNA damage similar to that of SN38, and derivatives **6** and **19** revealed an intensity of DNA cleavage only slightly inferior to SN38, whereas **24** and **25** were substantially less efficient.

The cleavage pattern was found similar to that of SN38 for all the new CPTs. The stabilization of the ternary cleavable complex was also evaluated after the addition of a high salt concentration (0.6 M NaCl), which favors the drug−enzyme−DNA complex dissociation. As shown in Figure 6B, the compounds revealed DNA damage persistence similar to that of SN38. The best activity was achieved with compound **6**. The introduction of the homospermidine produced a reduction in the persistence of DNA damage with respect to spermidine (**24** vs **6**). A reduced persistence was also observed in the presence of a spermine instead of a spermidine (compound **19** vs **6**). Compound **18** was the least effective in stabilizing the DNA damage.

Compounds **18**, **6**, and **24**, which bear different polyamines in position C21, were tested for their capability to bind the DNA by evaluating the reduced migration in agarose gel of SV40 DNA plasmid (Figure 7). In comparison to compound **18**, compounds **6** and **24** revealed the most dose-dependent reduced migration of DNA plasmid. This feature was dependent on the number of positive charges carried by the polyamine residue (one for compound **18** and two for compounds **6** and **24**). Of note, the DNA binding affinity was also influenced by the architecture of the polyamine chain (compare **24** vs **6**), since homospermidine introduction at the C21 position, instead of spermidine, increased the capability to interact with DNA.

Stability studies of compound **18** in cell culture medium and cleavage buffer solutions were conducted on the ESI generated ion 391.1938, in single ion monitoring (SIM) modality (see Materials and Methods for details and Figure 10 in the Supporting Information section for representative sample TIC and SIM chromatograms).

As shown in Table 2, compound **18** was stable after 1 h of incubation at 37 °C both in cell culture medium and in cleavage buffer, because a marginal content of CPT (about 3%) was observed in both conditions. Appreciable degradation of **18** was observed when the compound was incubated in cell culture medium for 72 h, with the appearance of a significant amount of CPT. When the experiments were performed in the presence of cells, after 1 h of treatment at the IC_{80} value, no CPT was

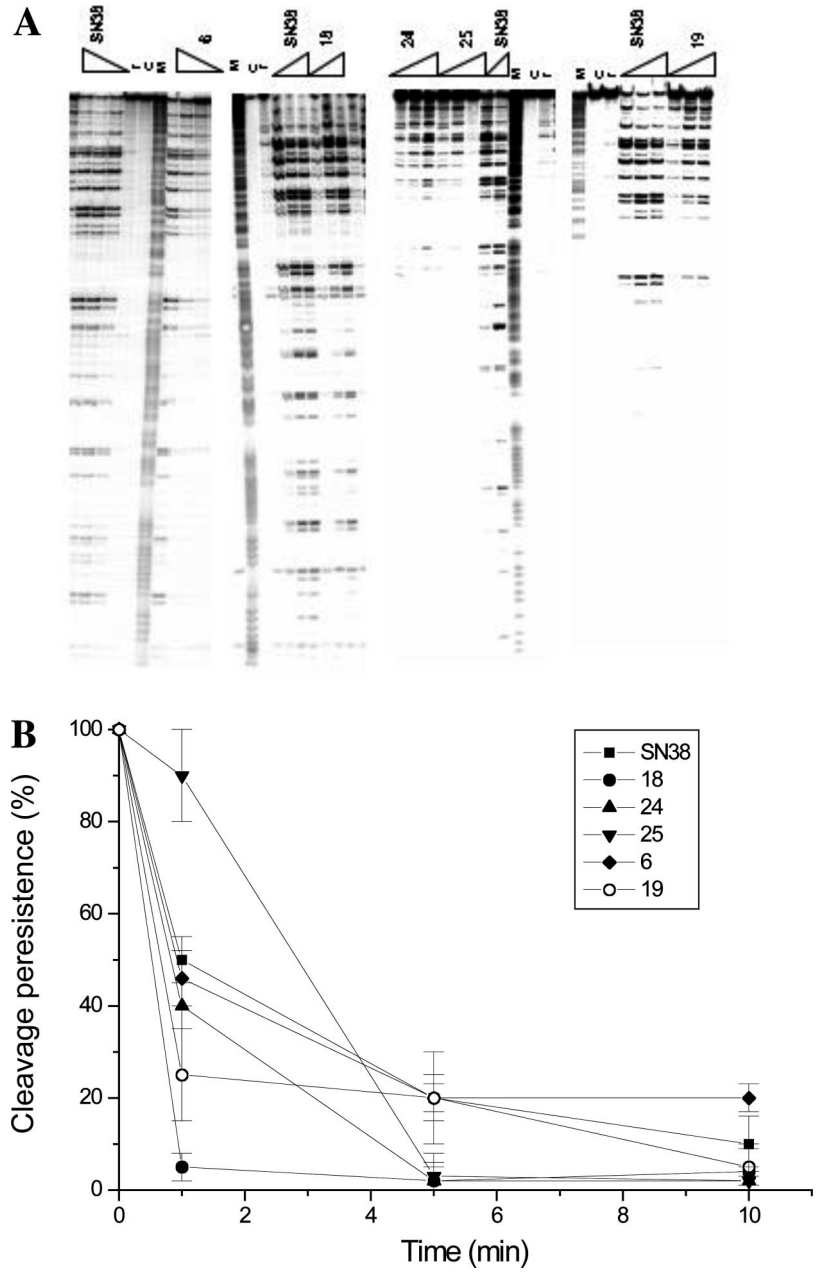

Figure 6. (A) Topoisomerase I-mediated DNA cleavage by SN38 and different camptothecin derivatives. Samples were reacted with 1, 10, and 50 μM drug at 37 °C for 30 min. Reaction was then stopped by adding 0.5% SDS and 0.3 mg/mL proteinase K and incubating for 45 min at 42 °C before loading on a denaturing 8% polyacrylamide gel. C, control DNA; T, reaction without drug; M, purine markers. (B) Persistence of topoisomerase I-mediated DNA cleavage in the presence of different compounds. The samples were reacted for 30 min with 10 μM drug in presence of top I. After this time, DNA damage was reversed by adding 0.6 M NaCl and incubating at 37 °C for 1, 5, and 10 min. The 100% value is referred to the extent of DNA cleavage at 30 min of incubation with top I. The experiment was repeated 3 times and the results of a representative value are reported.

found in the cell pellet; whereas a slight amount of CPT (3.7%) was recognized in cell culture medium (Table 2).

DISCUSSION AND CONCLUSION

The results reported in this study provide further evidence (*42*) that CPT polyamine conjugates with the open E-ring may be effective as cytotoxic agents and topo I inhibitors. Their activity was markedly dependent on the polyamine substituent. The introduction of suitable substituents in the open carboxylate form results in derivatives able to stabilize the cleavable complex. These CPT derivatives exhibited growth inhibition potency similar to or higher than that of topotecan, SN38, and CPT after long-term exposure. It is likely that the nature of the substituent is critical in promoting rapid intracellular drug accumulation and in achieving an optimal cytotoxic effect. Indeed, it is well-known that pharmacokinetic behavior at the cellular level is a critical determinant of the antitumor efficacy of CPTs, because as a consequence of the potential reversibility of the cleavable complex, adequate intracellular concentrations and exposure are required to produce a lethal extent of DNA damage. The growth inhibition potency during long-term exposure is correlated with the number of the charges of the substituent. Indeed, **18** was found the most active compound, while **25**, **24**, **19**, and **6**, which are the most charged derivatives, were the less active of the series. Interestingly, this pattern of activity was not observed after 1 h exposure for which, on the

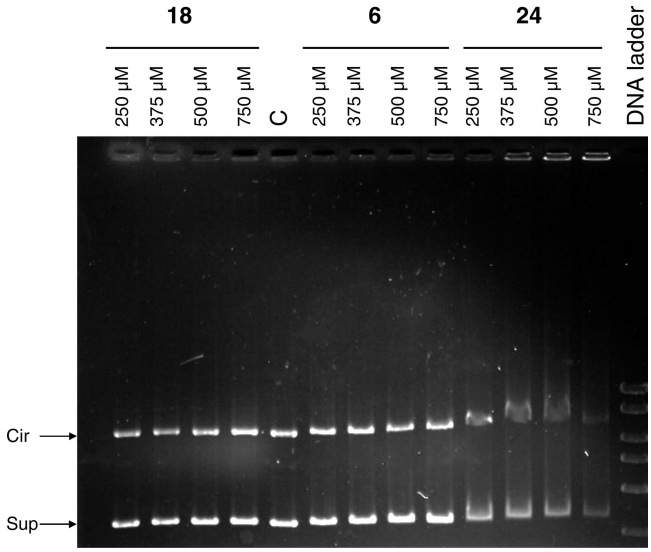

Figure 7. DNA binding of compounds **18**, **6**, and **24**. DNA and CPT analogues were incubated in 20 μL of phosphate buffered saline for 1 h at 37 °C in the presence of 100 ng of SV40 DNA plasmid at the indicated concentrations of compounds. Samples were analyzed on 0.7% agarose gel, followed by ethidium bromide staining. The arrows indicate the migration of the circular (Cir) and supercoiled (Sup) DNA plasmid.

Table 2. Stability of Compound 18[a]

experimental conditions		concentration (%)	
		18 (%)	CPT (%)
cell free conditions	medium (1 h)	96.4	3.6
	medium (72)	82.7	17.3
	cleavage buffer (1 h)	97.7	2.3
in presence of cells	medium (1 h)	96.3	3.7

[a] The amount of camptothecin produced by incubating compound **18** in different conditions was determined using LC/MS. The concentration of **18** added to cell culture medium or cleavage buffer was 50 μM. The experiments in presence of cells were performed by treating the cell culture at the IC_{80} value (about 60 μM) of **18** for 1 h and immediately harvesting both cell pellet and culture medium. The values are the means of three independent measures.

contrary, the most active derivative was **25**, which contains the longest polyamine side chain. The high antiproliferative activity observed for **18** after long-term exposure could suggest a major capability of this compound in promoting the E-ring closure, thus producing the structure of natural CPT. This feature is supported by an antiproliferative potency of **18** similar to that of CPT and by the formation of CPT (about 17%) after long-term incubation (72 h) in cell culture medium (Table 2). Thus, it is likely that, for this derivative, long-term exposure is required to produce E-ring closure. However, the cleavage assay and *in vitro* effects support the interpretation that the compounds may have inhibitory activity also in the open ring form. This feature is corroborated by the low amount of CPT (3.7%) observed incubating **18** for short-term exposure (1 h) in culture medium and by the absence of CPT recovered in the cells after this time exposure (Table 2). The architecture of the polyamine moiety is important for antiproliferative activity, and a balance between the hydrophilic and lipophilic properties of the polyamine is critical for CPT potency. The introduction of homospermidine instead of a spermidine in C21 reduced the antiproliferative effect after both short- and long-term exposure (compound **24** vs **6**). In addition, during short-term exposure, the potency seems to be correlated with the length of the polyamine, e.g., **25** versus topotecan; while during long-term exposure, a reduced potency was found for those compounds bearing long polyamine side chain. This observation supports a crucial role of the polyamine in the cellular pharmacokinetics.

The capability to stabilize the cleavable complex was found to be markedly dependent on the nature/length of the substituent linked to the 21-position of the CPT. Indeed, **24** and **25**, which carry a long polyamine moiety, displayed a low potency; on the contrary, **18** was very active in producing DNA damage. This feature appears independent from the capability of compound **18** to interact with the DNA in the absence of topo I (Figure 7) indicating that the ethyl-diamine moiety is more proficient than other substituents in fitting the CPT into the enzyme−DNA and thus producing more potent inhibition. Interestingly, reduced DNA damage was observed after exposure to a high concentration (50 μM) of **25** (Figure 6A). It is likely that this behavior is the result of the interaction between the long polyamine chain and the DNA substrate that, in so doing, inhibits the access of the enzyme into DNA sequences, thus reducing the cleavage efficacy of the compound. This hypothesis is also supported by the major capability of compounds **6** and **24** to interact with the DNA in the absence of topo I (Figure 7). Although of slight magnitude, compound **6** produced the more stable DNA damage, indicating that spermidine presents the best architecture for the interaction with the DNA in the presence of topo I. Our results support the efficacy per se of CPT with an open lactone ring in poisoning the topo I. Nevertheless, the antiproliferative activity and time-dependent effects probably reflect not only the inhibitory potency at target level but also the pharmacological behavior, which is determined by multiple and complex interactions, e.g., drug uptake, DNA interaction, and E-ring closure. The latter event could correlate with the properties of the polyamine moiety linked to the C21. Indeed, among the tested compounds, the most evident increase in cytotoxic potency found comparing short- and long-term exposure was observed for compound **18** (2600- vs 30-fold compared to CPT) that could indicate that the presence of an ethyl-diamine moiety may favor an efficient E-ring closure as a consequence of its easy release.

At concentrations of **18** required for cytotoxic effects during long-term exposure, the presence of free CPT was not measurable in cell culture medium. The expected amount on the basis of stability experiments (17%, Table 2) does not account for the activity reported in Table 1. Indeed, the potency of **18** is higher than that of CPT itself. In conclusion, although a contribution of CPT itself could not be ruled out, the available evidence supports that the CPT polyamine conjugates with the open E-ring may be active "per se".

Supporting Information Available: Figure 8, 9, 10, as described in the text, are provided. This material is available free of charge via the Internet at http://pubs.acs.org.

LITERATURE CITED

(1) Hsiang, Y.-H., Hertzberg, R., Hecht, S., and Liu, L. F. (1985) Camptothecin induces protein-linked DNA breaks via mammalian DNA topoisomerase I. *J. Biol. Chem. 260*, 14873–14878.

(2) Wang, J. C. (1996) DNA topoisomerases. *Annu. Rev. Biochem. 65*, 635–692.

(3) Champoux, J. J. (1998) Domains of human topoisomerase I and associated functions. *Prog. Nucleic Acid Res. Mol. Biol. 60*, 111–132.

(4) Wu, J. X., and Liu, L. F. (1997) Processing of topoisomerase I cleavable complexes into DNA damage by transcription. *Nucleic Acids Res. 25*, 4181–4186.

(5) Redinbo, M. R., Stewart, L., Kuhn, P., Champoux, J. J., and Hol, W. G. J. (1998) Crystal structures of human topoisomerase I in covalent and noncovalent complexes with DNA. *Science 279*, 1504–1513.

(6) Staker, B. L., Feese, M. D., Cushman, M., Pommier, Y., Zembower, D., Stewart, L., and Burgin, A. B. (2005) Structures of three classes of anticancer agents bound to the human topoisomerase I-DNA covalent complex. *J. Med. Chem. 48*, 2336–2345.

(7) Marchand, C., Antony, S., Kohn, K. W., Cushman, M., Ioanoviciu, A., Staker, B. L., Burgin, A. B., Lance Stewart, L., and Pommier, Y. (2006) A novel norindenoisoquinoline structure reveals a common interfacial inhibitor paradigm for ternary trapping of the topoisomerase I-DNA covalent complex. *Mol. Cancer Ther. 5*, 287–295.

(8) Sanna, N., Chillemi, G., Grandi, A., Castelli, S., Desideri, A., and Barone, V. (2005) New hints on the pH-driven tautomeric equilibria of the topotecan anticancer drug in aqueous solutions from an integrated spectroscopic and quantum-mechanical approach. *J. Am. Chem. Soc. 127*, 15429–15436.

(9) Bocian, W., Kawecki, R., Bednarek, E., Sitkowski, J., Pietrzyk, A., Williamson, M. P., Hansen, P. E., and Kozerski, L. (2004) Multiple binding modes of the camptothecin family to DNA oligomers. *Chem. Eur. J. 10*, 5776–5787.

(10) Fan, Y., Weinstein, J. N., Kohn, K. W., Shi, L. M., and Pommier, Y. (1998) Molecular modeling studies of the DNA-topoisomerase I ternary cleavable complex with camptothecin. *J. Med. Chem. 41*, 2216–2226.

(11) Kerrigan, J. E., and Pilch, D. S. (2001) A structural model for the ternary cleavable complex formed between human topoisomerase I, DNA, and camptothecin. *Biochemistry 40*, 9792–9798.

(12) Laco, G. S., Collins, J. R., Luke, B. T., Kroth, H., Sayer, J. M., Jerina, D. M., and Pommier, Y. (2002) Human topoisomerase I inhibition: Docking camptothecin and derivatives into a structure-based active site model. *Biochemistry 41*, 1428–1435.

(13) Lauria, A., Ippolito, M., and Almerico, A. M. (2007) Molecular docking approach on the Topoisomerase I inhibitors series included in the NCI anti-cancer agents mechanism database. *J. Mol. Modeling 13*, 393–400.

(14) Xiao, X., and Cushman, M. (2005) Effect of E-ring modifications in camptothecin on topoisomerase I inhibition: A quantum mechanics treatment. *J. Org. Chem. 70*, 9584–9587.

(15) Gupta, M., Fujimori, A., and Pommier, Y. (1995) Eukariotic DNA topoisomerases-I. *Biochim. Biophys. Acta 1262*, 1–14.

(16) Wall, M. E. (1969) *Biochemie und Physiologie der Alkaloide* (Mothes, K., and Schreiber, K., Eds.) pp 77−87, Akademie Verlag, Berlin.

(17) Slichenmeyer, W. J., Rowinsky, E. K., Donehower, R. C., and Kaufman, S. H. (1993) The current status of camptothecin analogs as antitumour agents. *J. Natl. Cancer Inst. 85*, 271–291.

(18) Wani, M. C., Nicholas, A. W., Manikumar, G., and Wall, M. E. (1987) Plant antitumor agents. Total synthesis oand antileukemic activity of ring A substituted camptothecin analogs. Structure activity correlations. *J. Med. Chem. 30*, 1774–1779.

(19) Giovanella, B. C., Hinz, H. R., Kozielski, A. J., Stehlin, J. S., Silber, R., and Potmesil, M. (1991) Complete growth-inhibition of human cancer xenografts in nude-mice by treatment with 20-(S)-camptothecin. *Cancer Res. 51*, 3052–3055.

(20) Fleury, F., Kudelina, I., and Nabiev, I. (1997) Interactions of lactone, carboxylate and self-aggregated forms of camptothecin with human and bovine serum albumins. *FEBS Lett. 406*, 151–156.

(21) Mi, Z., and Burke, T. G. (1994) Marked interspecies variations concerning the interactions of camptothecin with serum albumins - a frequency-domain fluorescence spectroscopic study. *Biochemistry 33*, 12540–12545.

(22) Kingsbury, W. D., Bohem, J C., Jakas, D. R., Holden, K. G., Hecht, S. M., Gallagher, G., Carafa, M. J., McCabe, F. L., Faucette, L. F., Johnson, R. K., and Hertzberg, R. P. (1991) Synthesis of water-soluble (aminoalkyl)camptothecin analogs - inhibition of topoisomerase-i and antitumor-activity. *J. Med. Chem. 34*, 98–107.

(23) Masuda, N., Fukuoka, Y., Kusunoki, K., Matsui, N., Takifuji, S., Kudoly, S., Negoro, M., Nishioka, K., Nakagawa, H., and Takada, J. (1992) A new derivative of camptothecin for the treatment of refractory or relapsed small-cell lung-cancer. *J. Clin. Oncol. 10*, 1225–1229.

(24) Macdonald, J. S., Benedetti, J. K., Modiano, M., and Alberts, D. S. (1997) Phase II evaluation of topotecan in patients with advanced colorectal cancer - A Southwest Oncology Group Trial (SWOG 9241). *Invest. New Drugs 15*, 357–359.

(25) Saltz, L. B., Schwartz, G. K., Ilson, D. H., Quan, V., and Kelsen, D. P. (1997) A phase II study of topotecan administered five times daily in patients with advanced gastric cancer. *Am. J. Clin. Oncol. 20*, 621–625.

(26) http://www.pharmcast.com/WarningLetters/Yr2003/Nov2003/Pfizer1103.htm.

(27) Dubowchik, G. M., and Walker, M. A. (1999) Receptor-mediated and enzyme-dependent targeting of cytotoxic anticancer drugs. *Pharmacol. Ther. 83*, 67–123.

(28) Huang, P. S., and Oliff, A. (2001) Drug-targeting strategies in cancer therapy. *Curr. Opin. Gen. Dev. 11*, 104–110.

(29) De Groot, F. M. H., Damen, E. W. P., and Scheeren, H. W. (2001) Anticancer prodrugs for application in monotherapy: Targeting hypoxia, tumor-associated enzymes, and receptors. *Curr. Med. Chem. 8*, 1093–1122.

(30) Fassberg, J., and Stella, V. J. (1992) A kinetic and mechanistic study of the hydrolysis of camptothecin and some analogs. *J. Pharm. Sci. 81*, 676–684.

(31) Zhao, H., Lee, C., Sai, P., Choe, Y. H., Boro, M., Pendri, A., Guan, S., and Greenwald, R. B. (2000) 20-O-acylcamptothecin derivatives: Evidence for lactone stabilization. *J. Org. Chem. 65*, 4601–4606.

(32) Yang, L.-X., Pan, X., and Wang, H.-J. (2002) Novel camptothecin derivatives. Part 1: Oxyalkanoic acid esters of camptothecin and their in vitro and in vivo antitumor activity. *Bioorg. Med. Chem. Lett. 12*, 1241–1244.

(33) Cao, Z., Harris, N., Kozielski, A., Vardeman, D., Stehlin, J. S., and Giovanella, B. (1998) Alkyl esters of camptothecin and 9-nitrocamptothecin: Synthesis, in vitro pharmacokinetics, toxicity, and antitumor activity. *J. Med. Chem. 41*, 31–37.

(34) De Groot, F. M. H., Busscher, G. F., Aben, R. W. M., and Scheeren, H. W. (2002) Novel 20-carbonate linked prodrugs of camptothecin and 9-aminocamptothecin designed for activation by tumour-associated plasmin. *Bioorg. Med. Chem. Lett. 12*, 2371–2376.

(35) Lerchen, H.-G., and Von dem Bruch, K. (2000) Synthesis of 20-O-linked 20(S)-camptothecin glycoconjugates: Impact of the side chain of the ester-linked amino acid on epimerization during the acylation reaction and on hydrolytic stability of the final glycoconjugates. *J. Prakt. Chem. 342*, 753–760.

(36) Prijovicha, Z. M., Leub, Y.-L., and Roffler, S. R. (2003) Stability of the new prodrug 9-aminocamptothecin glucuronide (9ACG) in the presence of human serum albumin. *Biochem. Pharmacol. 66*, 1181–1187.

(37) Matteucci, M., Lin, K.-Y., Huang, T., Wagner, R., Sternbach, D. D., Mehrotra, M., and Besterman, J. M. (1997) Sequence-specific targeting of duplex DNA using a camptothecin triple helix forming oligonucleotide conjugate and topoisomerase I. *J. Am. Chem. Soc. 119*, 6939–6940.

(38) Arimondo, P. B., Boutorine, A., Baldeyrou, B., Bailly, C., Kuwahara, M., Hecht, S. M., Sun, J.-S., Garestier, T., and Hélène, C. (2002) Design and optimization of camptothecin conjugates of triple helix-forming oligonucleotides for sequence-specific DNA cleavage by topoisomerase. *J. Biol. Chem. 277*, 3132–3140.

(39) Arimondo, P. B., Angenault, S., Halby, L., Boutorine, A., Schmidt, F., Monneret, C., Garestier, T., Sun, J.-S., Bailly, C., and Hélène, C. (2003) Spatial organization of topoisomerase I-mediated DNA cleavage induced by camptothecin-oligonucleotide conjugates. *Nucleic Acids Res. 31*, 4031–4040.

(40) Arimondo, P. B., Bailly, C., Boutorine, A., Ryabinin, V., Syniakov, A., Sun, J.-S., Garestier, T., and Hélène, C. (2001)

Directing topoisomerase I mediated DNA cleavage to specific sites by camptothecin tethered to minor- and major-groove ligands. *Angew. Chem., Int. Ed. 40*, 3045–3048.
(41) Wang, C. C., and Dervan, P. B. (2001) Sequence-specific trapping of Topoisomerase I by DNA binding polyamide-camptothecin conjugates. *J. Am. Chem. Soc. 123*, 8657–8661.
(42) Adamovics, J. A., and Hutchinson, C. R. (1979) Prodrug analogs of the anti-tumor alkaloid camptothecin. *J. Med. Chem. 3*, 310–314.
(43) Sawada, S., Yaegashi, T., Furuta, T., Yokokura, T., and Miyasaka, T. (1993) Chemical modification of an antitumor alkaloid, 20(S)-camptothecin: E-lactone ring-modified water-soluble derivatives of 7ethylcamptothecin. *Chem. Pharm. Bull. 41*, 310–313.
(44) Ogawa, T., Yaegashi,T., Sawada, S., Furuta, T. (2001) U.S. Patent 6,310,210 B1.
(45) Greenwald, R. B., Zhao, H., and Xia, J. (2003) Tripartate poly(ethylene glycol) prodrugs of the open lactone form of camptothecin. *Bioorg. Med. Chem. 11*, 2635–2639.
(46) This suggestion seems to be in contrast with literature results (*43*), claiming that the 17-OH-21-N^1,N^1-dimethylaminoethyl amide dipartates are not stable enough to survive cell tissue culture experiments, undergoing rapid cyclization to the lactone form at physiological pH. Hence, compound **4** should be *in vitro* active.
(47) Beretta, G. L., Petrangolini, G., De.Cesare, M., Pratesi, G., Perego, P., Tinelli, S., Tortoreto, M., Zucchetti, M., Frapolli, R., Bello, E., Manzotti, C., Fontana, G., Bombardelli, E., Battaglia, A., Samorì, C., and Zunino, F. (2006) Biological properties of IDN5174, a new synthetic camptothecin with the open lactone ring. *Cancer Res. 66*, 10976–10982.
(48) Cohen, S. S. (1998) *A Guide to the Polyamines*, Oxford University Press, Oxford.
(49) Igarashi, K., and Kashiwagi, K. (2000) Polyamines: Mysterious modulators of cellular functions. *Biochem. Biophys. Res. 271*, 559–564.
(50) Yoshida, M., Kashiwagi, K., Shigemasa, A., Taniguchi, S., Yamamoto, K., Makinoshima, H., Ishihama, A., and Igarashi, K. (2004) A unifying model for the role of polyamines in bacterial cell growth, the polyamine modulon. *J. Biol. Chem. 279*, 46008–46013.
(51) Cullis, P. M., Green, R. E., Merson.Davies, L., and Travis, N. (1999) Probing the mechanism of transport and compartmentalisation of polyamines in mammalian cells. *Chem. Biol. 6*, 717–729, and references therein.
(52) Bloomfield, V. A. (1997) DNA condensation by multivalent cations. *Biopolymers 44*, 269–282.
(53) Feuerstein, B. G., Williams, L. D., Basu, H. S., and Marton, L. J. (1991) Implications and concepts of polyamine-nucleic acid interactions. *J. Cell Biochem. 46*, 37–47.
(54) Kashiwagi, K., Yamaguchi, Y., Sakai, Y., Kobayashi, H., and Igarashi, K. (1990) Identification of the polyamine-induced protein as a periplasmic oligopeptide binding-protein. *J. Biol. Chem. 265*, 8387–8391.
(55) Fukuchi, J., Hiipakka, R. A., Kokontis, J. M., Nishimura, K., Igarashi, K., and Liao, S. (2004) TATA-binding protein-associated factor 7 regulates polyamine transport activity and polyamine analog-induced apoptosis. *J. Biol. Chem. 279*, 29921–29929.
(56) Uemura, T., Tachihara, K., Tomitori, H., Kashiwagi, K., and Igarashi, K. (2005) Characteristics of the polyamine transporter TPO1 and regulation of its activity and cellular localization by phosphorylation. *J. Biol. Chem. 280*, 9646–9652.
(57) Mani, K., Sandgren, S., Lilja, J., Cheng, F., Svensson, K., Persson, L., and Belting, M. (2007) HIV-Tat protein transduction domain specifically attenuates growth of polyamine deprived tumor cells. *Mol. Cancer Ther. 6*, 782–788.
(58) Vassylyev, D. G., Tomitori, H., Kashiwagi, K., Morikawa, K, and Igarashi, K. (1998) Crystal structure and mutational analysis of the *Escherichia coli* putrescine receptor. *J. Biol. Chem. 273*, 17604–17609.
(59) Phanstiel, O., IV, Price, H. L., Wang, L., Juusola, J., Kline, M., and Shah, S. M. (2000) The effect of polyamine homologation on the transport and cytotoxicity properties of polyamine-(DNA-intercalator) conjugates. *J. Org. Chem. 65*, 5590–5599.
(60) Wang, C., Delcros, J.-G., Cannon, L., Konate, F., Carias, H., Biggerstaff, J., Gardner, R. A., and Phanstiel, O. V. (2003) Defining the molecular requirements for the selective delivery of polyamine conjugates into cells containing active polyamine transporters. *J. Med. Chem. 46*, 5129–5138.
(61) Gardner, R. A., Delcros, J.-G., Konate, F., Breitbeil, I. I. I., Martin, B., Sigman, M., Huang, M., and Phanstiel, O. (2004) N-1-substituent effects in the selective delivery of polyamine conjugates into cells containing active polyamine transporters. *J. Med. Chem. 47*, 6055–6069.
(62) Phanstiel, O., IV, Kaur1, N., and Delcros, J.-G. (2007) Structure-activity investigations of polyamine-anthracene conjugates and their uptake via the polyamine transporter. *Amino Acids 33*, 305–313.
(63) Burns, M. R., Carlson, C. L., Vanderwerf, S. M., Ziemer, J. R., Weeks, R. S., Cai, F., Webb, H. K., and Graminski, G. F. (2001) Amino acid/spermine conjugates: Polyamine amides as potent spermidine uptake inhibitors. *J. Med. Chem. 44*, 3632–3644.
(64) Holley, J., Mather, A., Cullis, P., Symons, M. R., Wardman, P., Watt, R. A., and Cohen, G. M. (1992) Uptake and cytotoxicity of novel nitroimidazole-polyamine conjugates in ehrlich ascites tumor-cells. *Biochem. Pharmacol. 43*, 763–769.
(65) Siddiqui, A. Q., Merson-Davies, L., and Cullis, P. M. (1999) The synthesis of novel polyamine-nitroimidazole conjugates designed to probe the structural specificities of the polyamine uptake system in A549 lung carcinoma cells. *J. Chem. Soc., Perkin Trans. 1*, 3243–3252.
(66) Jakobs, A., Bernadou, J., and Meunier, B. (1997) Preparation of tetracationic metalloporphyrin - Spermine conjugates. *J. Org. Chem. 62*, 3505–3510.
(67) Rauter, H., Di.Domenico, R., Menta, E., Oliva, O., Qu, Y., and Farrell, N. (1997) Selective platination of biologically relevant polyamines. Linear coordinating spermidine and spermine as amplifying linkers in dinuclear platinum complexes. *Inorg. Chem. 36*, 3919–3927.
(68) Popaj, K., Guggisberg, A., and Hesse, M. (2000) Synthetic analogues to the spermidine-spermine alkaloid tenuilobine. *Helv. Chim. Acta 83*, 3021–3034.
(69) Dallavalle, S., Giannini, G, Alloatti, D., Casati, A., Marastoni, E., Musso, L., Merlini, L., Morini, G., Penco, S., Pisano, C., Tinelli, S., De.Cesare, M., Beretta, G. L., and Zunino, F. (2006) Synthesis and cytotoxic activity of polyamine analogues of camptothecin. *J. Med. Chem 49*, 5177–5186.
(70) Hu, V. W., and Hesse, M. (1996) The synthesis of p-Cumaroylspermidines. *Helv. Chim. Acta 79*, 548–559.
(71) Blagbrough, I. S., and Geall, A. J. (1998) Practical synthesis of unsymmetrical polyamine amides. *Tetrahedron Lett. 39*, 439–442.
(72) Bombardelli, E., and Verotta, L. (2000) U.S. Patent 6,121,277.
(73) Miller, K. A., Kumar, E. V. K. S., Wood, S. J., Cromer, J. R., Datta, A., and David, S. A. (2005) Lipopolysaccharide sequestrants: Structural correlates of activity and toxicity in novel acylhomospermines. *J. Med. Chem. 48*, 2589–2599.
(74) Marchesini, R., Colombo, A., and Caserini, C. (1996) Interaction of ionizing radiation with topotecan in two human tumor cell lines. *Int. J. Cancer 66*, 342–346.

BC800033R